

Gauss-Newton accelerated MPPI Control

Hannes Homburger* Katrin Baumgärtner** Moritz Diehl***
Johannes Reuter*

* *Institute of System Dynamics, HTWG Konstanz - University of Applied Sciences, 78462 Konstanz, Germany*
hhomburg@htwg-konstanz.de

** *Department of Microsystems Engineering (IMTEK), University of Freiburg, 79110 Freiburg, Germany*

*** *Department of Microsystems Engineering (IMTEK) and Department of Mathematics, University of Freiburg, 79110 Freiburg, Germany*

Abstract: Model Predictive Path Integral (MPPI) control is a sampling-based optimization method that has recently attracted attention, particularly in the robotics and reinforcement learning communities. MPPI has been widely applied as a GPU-accelerated random search method to deterministic direct single-shooting optimal control problems arising in model predictive control (MPC) formulations. MPPI offers several key advantages, including flexibility, robustness, ease of implementation, and inherent parallelizability. However, its performance can deteriorate in high-dimensional settings since the optimal control problem is solved via Monte Carlo sampling. To address this limitation, this paper proposes an enhanced MPPI method that incorporates a Jacobian reconstruction technique and the second-order Generalized Gauss-Newton method. This novel approach is called *Gauss-Newton accelerated MPPI*. The numerical results show that the Gauss-Newton accelerated MPPI approach substantially improves MPPI scalability and computational efficiency while preserving the key benefits of the classical MPPI framework, making it a promising approach even for high-dimensional problems.

Keywords: Model predictive control, Optimal control theory, Real-time optimal control

1. INTRODUCTION

Model Predictive Path Integral (MPPI) control is a sampling-based optimal feedback control method widely used in robotics applications (Kazim et al., 2024). Its theoretical foundation and its name originate from input-affine stochastic optimal control formulations, where the solution can be expressed as a *path integral* derived from the Feynman–Kac lemma (Kappen, 2005). Via an *information-theoretic* approach, the framework has been generalized to nonlinear dynamical systems (Williams et al., 2018) and is commonly used as a GPU-accelerated random search variant for deterministic optimal control problems, particularly arising in nonlinear model predictive control (NMPC), see Zhang et al. (2024) and Halder et al. (2025).

To model and simulate complex physical systems, simulation engines such as *Dart* (Lee et al., 2018), *MuJoCo* (Todorov et al., 2012), and *Isaac Sim* by NVIDIA are widespread tools. However, these engines often do not provide sensitivity information. Given the black-box nature of specific simulation engines, the MPPI control method offers desirable properties, including flexibility and robustness. These properties are exploited, e.g., by Sundaralingam and coauthors (2023) to solve optimal control problems using a simulation engine to represent the dynamics. Nevertheless, the performance of MPPI deteriorates in high-dimensional settings because the underlying sampling distribution can exhibit high variance, which can

lead to convergence issues, particularly when solving optimal control problems with long time horizons or unstable system dynamics.

To mitigate this limitation, various approaches have been proposed to enhance sampling efficiency. For example, learning more informative sampling distributions can increase the proportion of low-cost samples (Sacks and Boots, 2023). Furthermore, the use of learned basis skills within the MPPI framework has been investigated in Homburger et al. (2022) and later extended in Trevisan and Alonso-Mora (2024), which incorporated general ancillary controllers. Classical optimization methods have been applied to enhance sampling-based controllers. For example, path integral control has been enhanced through differential dynamic programming approaches (Lefebvre and Crevecoeur, 2019) and an uncertainty-aware MPPI variant has been leveraged with iterative linear-quadratic Gaussian control (Gandhi et al., 2021). A review of various developments is provided in Kazim et al. (2024). Although such methods mitigate sampling inefficiency to some extent, they remain fragile to the curse of dimensionality, manifested via the variance of the Monte Carlo estimator.

In the field of numerical optimization, second-order techniques such as the Generalized Gauss-Newton method (Schraudolph, 2002) are commonly employed to approximate the Hessian matrix within Newton-type optimization schemes that can be highly efficient and exploit the

problem’s structure (Rawlings et al., 2022, Sec. 8.6). In particular, the favorable local convergence properties of the Generalized Gauss-Newton method have been investigated by (Messerer et al., 2021, Sec. 2.3).

Contribution. In this work, we integrate Jacobian reconstruction techniques and the second-order Generalized Gauss-Newton method from numerical optimization into the MPPI control framework to improve its performance and scalability. The presented approach preserves the key properties of classical MPPI, given by its flexible interface and the parallel evaluation of the objective.

Structure. The remainder of this paper is organized as follows. Section 2 formulates the optimal control problem to be solved. Section 3 provides a review of the deterministic MPPI control approach. The proposed Gauss-Newton-accelerated MPPI method is introduced in Section 4 and compared with other optimization approaches in Section 5. Finally, Section 6 concludes the paper.

2. PROBLEM FORMULATION

Let us consider a deterministic black-box simulator $F : \mathbb{R}^{n_x} \times \mathbb{R}^{Nn_u} \rightarrow \mathbb{R}^{(N+1)n_x}$, which might be highly nonlinear or even nonsmooth, an initial state $\bar{x}_0 \in \mathbb{R}^{n_x}$, and a discrete-time N -step input trajectory $U = [u_0^\top, u_1^\top, \dots, u_{N-1}^\top]^\top \in \mathbb{R}^{Nn_u}$, then the state trajectory can be computed by

$$X = F(\bar{x}_0, U), \quad (1)$$

where $X = [x_0^\top, x_1^\top, \dots, x_N^\top]^\top \in \mathbb{R}^{(N+1)n_x}$ contains the simulated states $x_k \in \mathbb{R}^{n_x}$ for $k = 0, 1, \dots, N$.

Given an initial state \bar{x}_0 , the performance of a control trajectory U is described by the *overall costs* given by

$$C(\bar{x}_0, U) := \sum_{k=0}^{N-1} L_k(x_k(\bar{x}_0, U), u_k) + E(x_N(\bar{x}_0, U)), \quad (2)$$

where $L_k : \mathbb{R}^{n_x} \times \mathbb{R}^{n_u} \rightarrow \mathbb{R}_0^+$ for $k = 0, \dots, N-1$ are the stage costs and $E : \mathbb{R}^{n_x} \rightarrow \mathbb{R}_0^+$ is the terminal cost.

The optimal input trajectory for the corresponding deterministic, unconstrained, finite-horizon, and discrete-time optimal control problem is given by

$$U^*(\bar{x}_0) = \operatorname{argmin}_{U \in \mathbb{R}^{Nn_u}} C(\bar{x}_0, U), \quad (3)$$

where $U^* : \mathbb{R}^{n_x} \rightarrow \mathbb{R}^{Nn_u}$ is the optimal input trajectory.

We can express the objective (2) in the special structure

$$C(\bar{x}_0, U) = \Phi(R(\bar{x}_0, U)), \quad (4)$$

such that the objective is a composition of a nonlinear, unknown, and possibly nonsmooth *inner function* $R : \mathbb{R}^{n_x} \times \mathbb{R}^{Nn_u} \rightarrow \mathbb{R}^{n_R}$ and a *outer function* $\Phi : \mathbb{R}^{n_R} \rightarrow \mathbb{R}_0^+$. In case of L_k for all $k = 0, \dots, N-1$ and E convex, the outer function Φ is convex, and we obtain a *convex-over-unknown* cost structure in Eq. (4).

Note that the convex-over-unknown structure is typical in NMPC approaches, where the system dynamics are simulated using a black-box engine and the cost function is chosen to be convex. This structure is depicted in Figure 1.

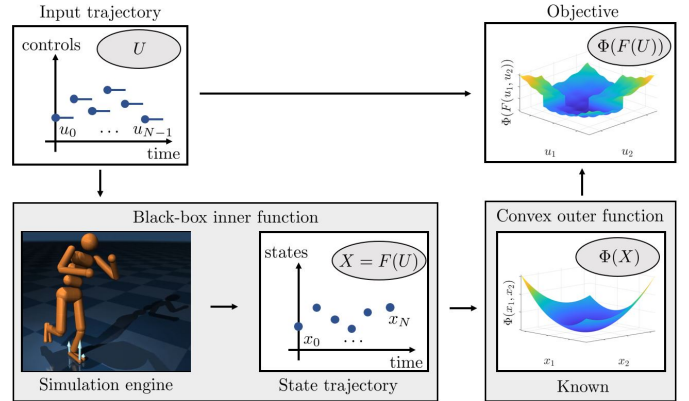


Fig. 1. Schematic visualization of the *convex-over-unknown* structure of the NLP objective in Eq. (4). For simplicity, the special case $R = X$ is considered.

3. DETERMINISTIC MPPI CONTROL

To solve the optimal control problem (3) numerically, the deterministic MPPI approach is based on the iterates $U_{k+1} = U_k + \Delta U_{\text{MPPI}}(U_k)$ with step $\Delta U_{\text{MPPI}}(U_k) =$

$$\frac{1}{\eta_k} \mathbb{E}_{W \sim \mathcal{N}(0, \Sigma_k)} \left[W \exp \left(-\frac{1}{\lambda_k} C(\bar{x}_0, U + W) \right) \right], \quad (5)$$

where $U_k \in \mathbb{R}^{Nn_u}$ is an initial guess, $W \in \mathbb{R}^{Nn_u}$ is a multivariate normal distributed random variable with mean zero and covariance Σ_k , the scalar

$$\eta_k = \mathbb{E}_{W \sim \mathcal{N}(0, \Sigma_k)} \left[\exp \left(-\frac{1}{\lambda_k} C(\bar{x}_0, U + W) \right) \right] \quad (6)$$

normalizes the distribution, and $\lambda_k > 0$ is a scalar tuning parameter, see e.g. the presentation by Yi et al. (2024). For the limit $\lambda_k \rightarrow 0$, the convergence of the deterministic MPPI method can be proven using Laplace’s method; see e.g. Thm. 1 in Homburger et al. (2025b) for a similar result. The basis for the application of the MPPI method is to approximate the expectation in Eq. (5) by the empirical mean calculated by a finite number of M samples

$$\Delta U_{\text{MPPI}}(U_k) \approx \frac{\sum_{m=1}^M [W_m \omega_m]}{\sum_{m=1}^M [\omega_m]}, \quad (7)$$

where

$$\omega_m := \exp \left(-\frac{1}{\lambda_k} C(\bar{x}_0, U_k + W_m) \right) \quad (8)$$

are the *sample weights* for $m = 1, \dots, M$ samples. Note that the presented deterministic MPPI approach in Eq. (5) is only one of many methods within the MPPI framework (Kazim et al., 2024). The essence of this framework is that the empirical weighted mean in Eq. (7) underlies most MPPI algorithms (cf., e.g., Williams et al. (2018); Kazim et al. (2024); Halder et al. (2025)). The samples and corresponding weights in Eq. (7) can be generated in parallel with algorithms tailored to GPUs (Vlahov et al., 2024). In general, MPPI does not require any sensitivity information. This allows MPPI to treat problems in a black-box setting.

3.1 Sample complexity analysis

The motivation for the approximation of the expectation by a weighted empirical mean in Eq. (7) is based on the

strong law of large numbers (Vershynin, 2018, Thm. 1.3.1). Now the question arises: how many samples are necessary to provide a good estimate using Eq. (7)? The following lemma is a standard result from Monte Carlo theory and provides a bound on the expected error in general Monte Carlo approaches that is dependent on the variance of the random variable and the number of samples in the empirical mean. Lemma 1 is adapted from Chapter 3 of the textbook by Vershynin (2018).

Lemma 1. (Monte Carlo error bound). Let X_1, X_2, \dots, X_n be i.i.d. random vectors in \mathbb{R}^{n_x} with mean $\mathbb{E}[X] = \mu$ and finite covariance matrix $\Sigma \succ 0$. Then for the empirical mean of n samples $\bar{X}_n := \frac{1}{n} \sum_{i=1}^n X_i$, it follows

$$\mathbb{E} \left[\|\bar{X}_n - \mu\|_2 \right] \leq \frac{\sqrt{\text{tr}(\Sigma)}}{\sqrt{n}}.$$

Sketch of proof: Let $Y = \bar{X}_n - \mu$ and note that $\text{Cov}(Y) = \frac{\Sigma}{n}$. The Jensen inequality for the Euclidean norm yields

$$\mathbb{E} [\|Y\|_2] \leq \sqrt{\mathbb{E} [\|Y\|_2^2]}.$$

By identifying

$$\mathbb{E} [\|Y\|_2^2] = \text{tr}(\text{Cov}(Y)) = \text{tr} \left(\frac{\Sigma}{n} \right) = \frac{\text{tr}(\Sigma)}{n},$$

the claimed result is immediate. \square

Note that the trace can be bounded by $\text{tr}(\Sigma) \leq n_x \bar{\lambda}$, where $\bar{\lambda}$ is the largest eigenvalue of Σ , which coincides with the largest diagonal entry if Σ is diagonal. The *strong law of large numbers* motivates the use of the empirical mean, and Lemma 1 quantifies the number of samples required to achieve a reliable approximation on average. Because the error bound scales as $\propto 1/\sqrt{n}$, obtaining an additional correct decimal digit requires increasing the sample size by a factor of 100. This convergence rate is slow, particularly for low-dimensional problems. The Monte-Carlo method’s “reason to be” lies in its straightforward applicability to multivariate random variables, where the decrease of the error bound holds regardless of dimensionality.

Note that tighter bounds can be established for specific applications of MPPI control (Yoon et al., 2022), e.g., in the linear quadratic regulator (LQR) case via Hoeffding’s inequality, the sample size required exhibits a logarithmic dependence on the dimension of the control input trajectory (Patil et al., 2024, Sec. 4.A).

3.2 Properties of the MPPI algorithm

The MPPI solution Eq. (7) relies solely on evaluations of the objective C , which embeds the simulator’s black-box dynamics, requiring no gradient or Hessian information and making it easy to implement. This allows MPPI to handle problems where sensitivities are unavailable. MPPI is also robust to poor initial guesses, as even a single low-cost sample can guide the update. See Kazim et al. (2024) for a detailed discussion.

Despite the presented benefits of MPPI approaches, the algorithm completely ignores the internal problem structure of the optimal control problem and first- and second-order information that is valuable to exploit in most problem formulations (Rawlings et al., 2022, Sec. 8). Exploiting the

structure of the problem and the information of first and second-order is a key element to achieve fast convergence in Newton-type optimization algorithms tailored to the problem structure (Baumgärtner et al., 2023).

Facing the different approaches, the question arises whether it is possible to combine the benefits of both methods and achieve faster convergence by using structured evaluations of the cost function rather than purely sampling.

4. GAUSS-NEWTON ACCELERATED MPPI

In this section, we introduce the Gauss-Newton accelerated MPPI method. We start by reviewing techniques to reconstruct Jacobian information from black-box functions. Then, the Gauss-Newton accelerated MPPI algorithm is presented. In the remainder of this paper, we omit the parameter dependency on the initial state in the notation, e.g., we will use $C(U) \equiv C(\bar{x}_0, U)$ and $R(U) \equiv R(\bar{x}_0, U)$ for readability.

4.1 Jacobian reconstruction

The Generalized Gauss-Newton approach is based on the Jacobian of the unknown residuum function R . To reconstruct Jacobian information from black-box functions, several approaches have been proposed in the literature. We select the *Gaussian smoothing* method because it relies on a similar Gaussian-distributed function evaluation as standard MPPI, and it is applicable even if the unknown inner function is possibly nonsmooth.

Jacobian reconstruction by Gaussian smoothing. To approximate the Jacobian of the unknown inner function R , the function R can be treated by *Gaussian smoothing*, resulting in a smooth function

$$\hat{R}(U_k) = \mathbb{E}_{W \sim \mathcal{N}(0, \Sigma)} [R(U_k + W)], \quad (9)$$

where $\Sigma \succ 0$ is a diagonal positive definite covariance matrix (cf. Sec. 2.3 in Berahas et al. (2022)). The influence of the covariance is depicted in Figure 2. By exploiting properties of derivatives of the expectation (Asmussen and Glynn, 2007), we obtain the Jacobian as expectation

$$\frac{\partial \hat{R}}{\partial U}(U_k) = \mathbb{E}_{W \sim \mathcal{N}(0, \Sigma)} [R(U_k + W)W^\top] \Sigma^{-1}. \quad (10)$$

By assuming the existence of the Jacobian $\frac{\partial R}{\partial U}(U_k)$, it can be recovered by $\frac{\partial \hat{R}}{\partial U}(U_k)$ for $\|\Sigma\| \rightarrow 0$ (cf. Eq. (2.10) in Berahas et al. (2022)). The expectation can be approximated by Monte Carlo sampling with $M \in \mathbb{N}$ samples. This results in the computational complexity

$$\text{cost} \left(\frac{\partial \hat{R}}{\partial U}(U_k) \right) \approx M \cdot \text{cost}(R(U_k)) \quad (11)$$

that can be accelerated by execution in parallel, such that

$$\text{cost}_{\text{GPU}} \left(\frac{\partial \hat{R}}{\partial U}(U_k) \right) \approx \left\lceil \frac{M}{M_{\text{GPU}}} \right\rceil \cdot \text{cost}(R(U_k)) \quad (12)$$

follows under the hard assumption of ideal parallelization of $M_{\text{GPU}} \in \mathbb{N}$ processing units. We can approximate the Jacobian $J(U_k) := \frac{\partial R}{\partial U}(U_k)$ of the smoothed *inner* black-box function R of (4). Note that in the case of a differentiable inner function R , finite differences (Curtis et al., 1974) is another approach to approximate the Jacobian.

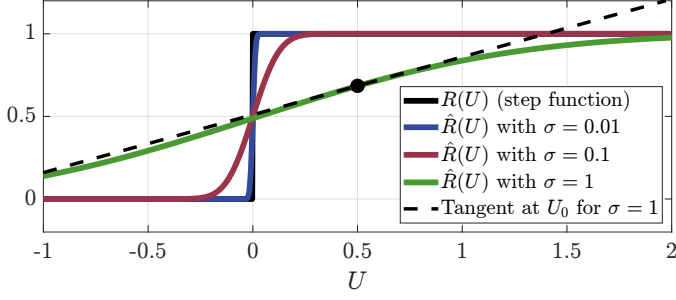


Fig. 2. Heaviside step function and Gaussian smoothed approximations, here scalar $\Sigma = \sigma^2$ with $\sigma > 0$.

4.2 Generalized Gauss-Newton (GGN) method

The Generalized Gauss-Newton (GGN) method (Schraudolph, 2002) is an iterative second-order optimization approach applicable to costs with a convex-over-nonlinear structure, as in Eq. (4), which is commonly used in NMPC applications.

Within the GGN method, the next iterate is computed as

$$U_{k+1} = U_k - \underbrace{B_{\text{GGN}}(U_k)^{-1} \nabla[\Phi(R(U_k))]}_{=: \Delta_{\text{GGN}}(U_k)}, \quad (13)$$

that is the minimizer of the convex quadratic *GGN subproblem*

$$\operatorname{argmin}_{U \in \mathbb{R}^{n_u}} \nabla[\Phi(R)]^\top (U - U_k) + \frac{1}{2} (U - U_k)^\top B_{\text{GGN}} (U - U_k),$$

where $\nabla[\Phi(R)]^\top = J^\top \nabla[\Phi](R)$ and the GGN Hessian is

$$B_{\text{GGN}}(U_k) := J(U_k)^\top \nabla^2 \Phi(R(U_k)) J(U_k) \succ 0.$$

The error of the GGN Hessian approximation with respect to the exact Hessian is

$$\nabla^2[\Phi(R(U))] - B_{\text{GGN}}(U) = \sum_{j=1}^{n_R} \nabla^2 R_j(U) \nabla_{R_j} \Phi(R(U)),$$

and contains the potentially indefinite terms of the Hessian of the original objective. Fast convergence is achieved when the curvature of the inner functions is small. See (Messerer et al., 2021, Sec. 2.3) for a detailed investigation of the convergence properties of the GGN method.

4.3 Gauss-Newton accelerated MPPI algorithm

Now the presented parts are put together to obtain the Gauss-Newton accelerated MPPI method that is summarized in Algorithm 1.

First, the Jacobian $J(U_k)$ is approximated using Gaussian smoothing, with M parallel evaluations of the inner function R . Based on this approximation, the full GGN step

Algorithm 1 Gauss-Newton accelerated MPPI

Require: Initial guess U_0 , maximum number of iterations K , number of samples M , initial covariance Σ_0 , shrinking rate β , step-length set \mathcal{A}

```

1: for  $k \in \{0, 1, \dots, K-1\}$  do
2:    $J_k \leftarrow \text{GETJACOBIAN}(U_k, \Sigma_k, M)$   $\triangleright$  Parallel smoothing (10)
3:    $\Delta_{\text{GGN}} \leftarrow -B_{\text{GGN}}(U_k)^{-1} \nabla \Phi(R(U_k))$   $\triangleright$  Full GGN step (13)
4:    $\alpha^* \leftarrow \text{LINESEARCH}(U_k, \Delta_{\text{GGN}}, \mathcal{A})$   $\triangleright$  Parallel sol. to (15)
5:    $U^{k+1} \leftarrow \text{GGNSTEP}(U_k, \Delta_{\text{GGN}}, \alpha^*)$   $\triangleright$  Apply GGN step (14)
6:    $\Sigma_{k+1} \leftarrow \beta \Sigma_k$   $\triangleright$  Shrink covariance
7: return  $U^* \leftarrow U_K$   $\triangleright$  Solution to (3)

```

is computed, after which, a standard line search method is employed to adjust the length of the GGN step (13) for globalization. This results in the iterative expression

$$U_{k+1} = U_k - \alpha^* B_{\text{GGN}}(U_k)^{-1} \nabla[\Phi(R(U_k))], \quad (14)$$

where the optimal step length α^* is selected by

$$\alpha^* = \operatorname{argmin}_{\alpha \in \mathcal{A}} C(U_k - \alpha B_{\text{GGN}}(U_k)^{-1} \nabla[\Phi(R(U_k))]), \quad (15)$$

where $\mathcal{A} = \{\gamma^k | k = 0, \dots, M-1\}$ is a set containing $M < M_{\text{GPU}}$ applicable step lengths with $\gamma \in (0, 1)$. The computation of the optimal step length can be executed in parallel, leading to a computational cost

$$\text{cost}_{\text{GPU}}(\alpha^*) \approx \text{cost}(C(U_k)) \approx \text{cost}(R(U_k)). \quad (16)$$

Finally, the covariance used for Gaussian smoothing can be reduced to improve the accuracy of the Jacobian approximation in the subsequent iteration.

Computing the Jacobian in Eq. (12) is necessary to determine the step direction in Eq. (13), and the step length in Eq. (15) can be optimized only after this direction has been obtained. Therefore, the overall computational cost of a Gauss-Newton accelerated MPPI step in parallel execution is roughly twice the cost of one evaluation of the inner function given in Eq. (1). The overall computational cost for K steps in Algorithm 1 is roughly

$$\text{cost}_{\text{GPU}}(\text{Algo. 1}) \approx 2K \cdot \left[\frac{M}{M_{\text{GPU}}} \right] \cdot \text{cost}(R(U_k)). \quad (17)$$

Note that the computational cost estimates are derived under the assumption that the computational cost of the simulator Eq. (1) dominates that of all other algorithmic components.

5. NUMERICAL EXPERIMENTS

To investigate the performance of the presented approaches, the following optimization problems are implemented in *convex-over-unknown* fashion, i.e., the inner functions do not provide any sensitivity information.

Problem I: Rosenbrock function. The objective is

$$\Phi(R(U)) = (1 - u_1)^2 + 100 (u_2 - u_1^2)^2$$

with inner function $R(U) = [\sqrt{2}(1-u_1), \sqrt{200}(u_2 - u_1^2)]^\top$ and outer function $\Phi(R) = \frac{1}{2} R R^\top$. The decision variable is $U = (u_1, u_2)$ and we use the initial guess $U_0 = (0, 0)$.

Problem II: Rastrigin function. The objective is given by

$$\Phi(R(U)) = 10 + u_1^2 - 5 \cos(2\pi u_1) + u_2^2 - 5 \cos(2\pi u_2)$$

with decision variable $U = (u_1, u_2)$. Problem II and the corresponding GGN subproblems are depicted in Figure 3. We use the initial guess $U_0 = (1.9, 1.7)$.

Problem III: Heaviside function. The inner function is

$$R(U) = \begin{cases} 1, & \text{for } u \geq 0 \\ 0, & \text{for } u < 0 \end{cases}$$

and the outer function is $\Phi = \frac{1}{2} R^2$ with decision variable $U = u \in \mathbb{R}$. We use the initial guess $U_0 = 0.5$.

Problem IV: Linear optimal control of a double integrator. Discrete time dynamics $x_{k+1} = Ax_k + Bu_k$ for $k = 0, \dots, N-1$ with $N \in \mathbb{N}$ and initial condition $x_0 = \bar{x}_0 \in \mathbb{R}^2$. The cost function is given by the quadratic costs $L(x_k, u_k) = x_k^\top Q x_k + u_k^\top R u_k$ and $E(x_N) = x_N^\top Q_N x_N$ with $Q, R, Q_N \succ 0$. We choose $N = 50$ steps and $U_0 = 0_{1 \times 50}$.

Problem V: Nonlinear optimal control of the (nonsmooth) Furuta pendulum. The dynamics are given by a black-box implementation of Eq. (2) in Homburger et al. (2025a). The task is to track a reference trajectory over $N = 20$ time steps, penalizing both tracking error and control effort. We distinguish between *Setting V.i*, where the standard dynamics are employed, and *Setting V.ii*, where we add the simple nonsmooth friction model

$$u_{k,\text{apply}} = \begin{cases} 0, & \text{for } |u_k| \leq u_{\text{friction}} \\ u_k, & \text{else} \end{cases}$$

at the input of the dynamical system. For both settings, the explicit RK4 method is used to discretize the smooth dynamics, and the nonsmooth friction model is applied to the discrete-time dynamics.

For comparison, each of the problems is solved with the following four methods:

Method A: GGN with *central finite difference* approximation of the Jacobian of R in mode with small perturbations $\epsilon \approx 1.49 \times 10^{-8}$ (Berahas et al., 2022, Eq. 1.2).

Method B: Gradient Descent. The gradient ∇C of the objective Eq. (2) is approximated using finite differences and determines the step in the descent direction.

Method C: Deterministic MPPI, as presented in Sec. 3.

Method D: Gauss-Newton accelerated MPPI (cf. Algo. 1) with random sampling of Eq. (10).

Method E: Gauss-Newton accelerated MPPI (cf. Algo. 1) with deterministic *Dirac-mixture* approximation of Eq. (10). This technique is based on the sigma-point approach utilized in the Unscented Kalman Filter (UKF) (Wan and Van Der Merwe, 2000).

For Methods C and D, $M = 2000$ samples with $\lceil M/M_{\text{GPU}} \rceil = 1$ are used, and antithetic sampling is employed to improve performance, cf. Sec. 4.2 in Glasserman (2003). For reproducibility, the full implementation is provided in the repository: `tba -- after publication`.

5.1 Results

The results obtained by applying the different methods to the control problems are presented in Table 1. Each entry in the table is encoded as

$$\left[\begin{array}{c} \{1, \dots, 1000\} \\ \{\checkmark, -, \times\} \end{array} \right] \equiv \left[\begin{array}{c} \text{number of iterations} \\ \{\text{opt. sol., subopt. sol., no sol.}\} \end{array} \right].$$

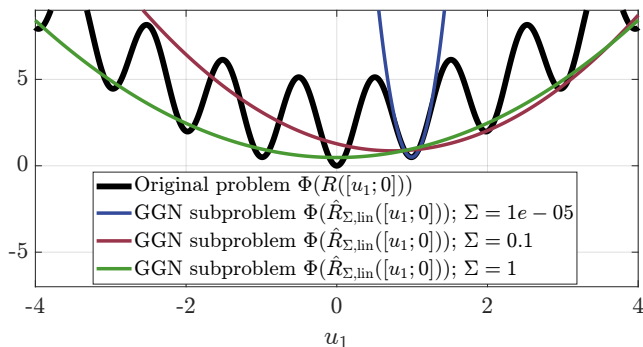


Fig. 3. Visualization of Problem II with u_2 fixed at 0. The GGN subproblems are expanded at $\hat{u}_1 = 0.9$. For small values of Σ , the GGN subproblem matches the original objective, while for larger Σ , the smoothed subproblem guides toward the global optimum.

Table 1. Results of the numerical experiments.

Method	A	B	C	D	E
Pr. I	12 ✓	1000 ×	17 ✓	14 ✓	12 ✓
Pr. II	3 –	4 –	7 ✓	4 ✓	2 ✓
Pr. III	not admissible	not admissible	2 ✓	2 ✓	2 ✓
Pr. IV	2 ✓	42 ✓	45 ✓	7 ✓	2 ✓
Pr. V.i	3 ✓	681 ✓	48 ✓	5 ✓	3 ✓
Pr. V.ii	not admissible	not admissible	50 ✓	6 ✓	3 ✓

The optimization is stopped if the step length and the (smoothed) gradient of the objective fall below a small threshold. The iteration count is a suitable indicator of computational effort, since each method requires two sequential evaluations of the inner function.

The results show that the GGN method with finite differences (Method A) achieves fast convergence in well-posed problem settings such as the Rosenbrock function and linear or nonlinear MPC with smooth objective functions. However, it converges only to a suboptimal solution for the Rastrigin function and is not admissible for optimizing nonsmooth problems with vanishing gradients. The gradient descent method with finite differences (Method B) generally requires a large number of iterations to converge (see, however, Problem II). It fails to solve the Rosenbrock function within 1000 iterations.

In contrast, the deterministic MPPI method (Method C) and the Gauss-Newton accelerated MPPI methods (Variant D and E) converge across all tested problem classes. In particular, Method E consistently achieves faster convergence (up to $\times 21$ fewer iterations), especially in high-dimensional settings (cf. Problems IV, V.i, and V.ii) compared to deterministic MPPI (Method C). Note that the deterministic MPPI method requires 45 iterations for the linear optimal control example (Problem IV), even though this problem is a quadratic program that could be solved in a single Newton step. Remember the limitation of the presented Gauss-Newton accelerated MPPI approach given by the restriction to the convex-over-unknown problem structure (4). However, as previously discussed, this structure is widespread in optimal control applications.

6. CONCLUSION

This paper introduces the *Gauss-Newton accelerated MPPI method*, which combines the complementary strengths of sampling-based and second-order optimization techniques. The numerical results demonstrate that the flexibility of MPPI for solving black-box problems is retained, while the rapid convergence properties of the Generalized Gauss-Newton (GGN) method can be effectively exploited. The proposed approach is well-suited for high-dimensional, unconstrained optimal control problems with a *convex-over-unknown* objective structure. This setting commonly arises when system dynamics are represented by black-box simulation engines.

ACKNOWLEDGEMENTS

The authors express their sincere gratitude to Prof. Dr. Oliver Dürr for our discussions on Monte Carlo methods.

REFERENCES

- Asmussen, S. and Glynn, P.W. (2007). *Stochastic Simulation: Algorithms and Analysis*, volume 57 of *Stochastic Modeling and Applied Probability*. Springer, New York.
- Baumgärtner, K., Messerer, F., and Diehl, M. (2023). A unified local convergence analysis of differential dynamic programming, direct single shooting, and direct multiple shooting. In *2023 European Control Conf. (ECC)*, 1–7.
- Berahas, A.S., Cao, L., Choromanski, K., and Scheinberg, K. (2022). A theoretical and empirical comparison of gradient approximations in derivative-free optimization. *Found. of Comp. Math.*, 22(2), 507–560.
- Curtis, A.R., Powell, M.J.D., and Reid, J.K. (1974). On the estimation of sparse jacobian matrices. *IMA Journal of Applied Mathematics*, 13(1), 117–119.
- Gandhi, M.S., Vlahov, B., Gibson, J., Williams, G., and Theodorou, E.A. (2021). Robust model predictive path integral control: Analysis and performance guarantees. *IEEE Rob. and Autom. Letters*, 6(2), 1423–1430.
- Glasserman, P. (2003). *Monte Carlo Methods in Financial Engineering*, volume 53 of *Springer eBook Collection Mathematics and Statistics*. Springer, New York, NY.
- Halder, P., Homburger, H., Kiltz, L., Reuter, J., and Althoff, M. (2025). Trajectory planning with signal temporal logic costs using deterministic path integral optimization. In *Proceedings of the IEEE Int. Conf. on Rob. and Autom. (ICRA)*, 4221–4228. IEEE. doi:10.1109/ICRA55743.2025.11127582.
- Homburger, H., Frey, J., Wirtensohn, S., Diehl, M., and Reuter, J. (2025a). Millisecond NMPC for swing-up and stabilization of the Furuta pendulum in real world. *IEEE Trans. on Control Systems Technology*, 1–7. doi:10.1109/TCST.2025.3616367.
- Homburger, H., Messerer, F., Diehl, M., and Reuter, J. (2025b). Optimality and suboptimality of MPPI control in stochastic and deterministic settings. *IEEE Control Systems Letters*, 9, 763–768. doi:10.1109/LCSYS.2025.3574151.
- Homburger, H., Wirtensohn, S., Diehl, M., and Reuter, J. (2022). Feature-based MPPI control with applications to maritime systems. *Machines*, 10(10), 1–23.
- Kappen, H.J. (2005). Path integrals and symmetry breaking for optimal control theory. *J. of Statistical Mechanics: Theory and Experiment*, 2005(11).
- Kazim, M., Hong, J., Kim, M.G., and Kim, K.K.K. (2024). Recent advances in path integral control for trajectory optimization: An overview in theoretical and algorithmic perspectives. *Annual Reviews in Control*, 57.
- Lee, J., Grey, M.X., Ha, S., Kunz, T., Jain, S., Ye, Y., Srinivasa, S.S., Stilman, M., and Liu, C.K. (2018). Dart: Dynamic animation and robotics toolkit. *J. of Open Source Software*, 3(22), 500. doi:10.21105/joss.00500.
- Lefebvre, T. and Crevecoeur, G. (2019). Path integral policy improvement with differential dynamic programming. In *Proc. of the IEEE/ASME Int. Conf. on Advanced Intelligent Mechatronics*, 739–745.
- Messerer, F., Baumgärtner, K., and Diehl, M. (2021). Survey of sequential convex programming and generalized Gauss-Newton methods. *ESAIM: Proceedings and Surveys*, 71, 64–88. doi:10.1051/proc/202171107.
- Patil, A., Hanasusanto, G.A., and Tanaka, T. (2024). Discrete-time stochastic LQR via path integral control and its sample complexity analysis. *IEEE Control Systems Letters*, 8, 1595–1600. doi:10.1109/LCSYS.2024.3413869.
- Rawlings, J.B., Mayne, D.Q., and Diehl, M.M. (2022). *Model Predictive Control: Theory, Computation, and Design*. Nob Hill Publishing, LLC, 2 edition.
- Sacks, J. and Boots, B. (2023). Learning sampling distributions for model predictive control. In A. Orthey and V. Berenz (eds.), *Proceedings of The 6th Conf. on Robot Learning*, volume 205 of *Proceedings of Machine Learning Research*, 1733–1742. PMLR.
- Schraudolph, N.N. (2002). Fast curvature matrix-vector products for second-order gradient descent. *Neural Computation*, 14(7), 1723–1738.
- Sundaralingam, B. and coauthors (2023). Curobo: Parallelized collision-free robot motion generation. In *2023 IEEE Int. Conf. on Rob. and Autom. (ICRA)*, 8112–8119. IEEE. doi:10.1109/ICRA48891.2023.10160765.
- Todorov, E., Erez, T., and Tassa, Y. (2012). MuJoCo: A physics engine for model-based control. In *2012 IEEE/RSJ Int. Conf. on Intelligent Robots and Systems (IROS)*, 5026–5033. IEEE. doi:10.1109/IROS.2012.6386109.
- Trevisan, E. and Alonso-Mora, J. (2024). Biased-MPPI: Informing sampling-based model predictive control by fusing ancillary controllers. *IEEE Rob. and Autom. Letters*, 9(6), 5871–5878.
- Vershynin, R. (2018). *High-dimensional probability: An introduction with applications in data science*, volume 47 of *Cambridge series in statistical and probabilistic mathematics*. Cambridge University Press, Cambridge.
- Vlahov, B., Gibson, J., Gandhi, M., and Theodorou, E.A. (2024). MPPI-generic: A CUDA library for stochastic optimization. *arXiv preprint arXiv:2409.07563*. doi:10.48550/arXiv.2409.07563.
- Wan, E.A. and Van Der Merwe, R. (2000). The unscented kalman filter for nonlinear estimation. In *Proceedings of the IEEE 2000 Adaptive Systems for Signal Proces., Comm., and Cont. Symp.*, 153–158.
- Williams, G., Drews, P., Goldfain, B., Rehg, J.M., and Theodorou, E.A. (2018). Information-theoretic model predictive control: Theory and applications to autonomous driving. *IEEE Trans. on Rob.*, 34(6), 1603–1622.
- Yi, Z., Pan, C., He, G., Qu, G., and Shi, G. (2024). CoVO-MPC: Theoretical analysis of sampling-based MPC and optimal covariance design. In *Proc. of the 6th Annual Learn. for Dyn. & Control Conf.*, volume 242, 1122–1135. PMLR.
- Yoon, H.J., Tao, C., Kim, H., Hovakimyan, N., and Voulgaris, P. (2022). Sampling complexity of path integral methods for trajectory optimization. In *2022 American Control Conf. (ACC)*, 3482–3487. IEEE. doi:10.23919/ACC53348.2022.9867607.
- Zhang, Y., Pezzato, C., Trevisan, E., Salmi, C., Corbato, C.H., and Alonso-Mora, J. (2024). Multi-modal MPPI and active inference for reactive task and motion planning. *IEEE Rob. and Autom. Letters*, 9(9), 7461–7468. doi:10.1109/LRA.2024.3426183.